3482 *Chem. Mater.* **2010,** *22,* 3482–3495
DOI:10.1021/cm1006108

CHEMISTRY OF MATERIALS
Article

The Role of Template Structure and Synergism between Inorganic and Organic Structure Directing Agents in the Synthesis of UTL Zeolite

Oleksiy V. Shvets,[†,‡] Natalia Kasian,[‡] Arnošt Zukal,[†] Jiří Pinkas,[†] and Jiří Čejka*[,†]

[†]*J. Heyrovský Institute of Physical Chemistry, Academy of Sciences of Czech Republic, v.v.i. Dolejškova 3, 182 23 Prague 8, Czech Republic, and* [‡]*L.V. Pisarzhevsky Institute of Physical Chemistry, National Academy of Sciences of Ukraine, Pr. Nauky 31, 03037 Kyiv, Ukraine*

Received February 27, 2010. Revised Manuscript Received April 12, 2010

The extra-large-pore germanosilicates with UTL topology have been synthesized using a large variety of spiroazocompounds as structure-directing agents. Synthesis conditions were optimized and zeolites with a high crystallinity degree were obtained with 13 different organic structure-directing agents. The influence of the composition of the reaction mixture and template nature (structure, hydrophilicity/hydrophobicity balance, rigidity, pK_a) on the phase selectivity, crystallinity degree, and adsorption properties of zeolites with UTL structure was investigated. Selection criteria of organic molecules as potential structure-directing agents (SDAs) in the synthesis of large-pore and extra-large-pore zeolites from silicate and germanosilicate media are proposed. The optimum synthesis time was determined to be 4−9 days for different SDA and (Si + Ge)/SDA molar ratios. Clear synergism between the optimum structure of organic template and the presence of critical amount of inorganic component (GeO_2) was evidenced. The UTL zeolite crystallizes as tiny sheets ∼10 μm thick. The effect of the organic template on the size and shape of the crystals was found. The micropore volume of the best crystals is 0.22−0.24 cm^3/g, with a micropore diameter of 1.05 nm, based on density functional theory (DFT), and Saito−Foley analyses of adsorption isotherms.

Introduction

Zeolite molecular sieves are the most frequently employed heterogeneous catalysts used in chemical industry,[1] because of important features such as having well-defined structures with micropore channels, chemical compositions that are able to introduce catalytic active centers, and environmental tolerance.[2] For the practical application of zeolites in acid catalysis, two particular features must be considered: (i) the size of the channels inducing the accessibility of active sites and (ii) the presence of acid sites (Brönsted and Lewis types), because of the successful incorporation of trivalent heteroatoms into the neutrally charged silica framework. The size of the zeolitic channels is sufficiently large for many transformations of aromatic hydrocarbons via alkylation, disproportionation, and isomerization reactions[3−9] or acylation reactions.[10,11] However, any increase in the size of channels above 1 nm would be surely desirable. As for the acidity, the investigation of acidic properties of zeolites is still a matter of highly vivid discussion, combining both experimental and theoretical approaches.[12−17]

Successful synthesis of new extra-large pore zeolites comprises the optimum application of organic structure-directing agents, proper synthesis conditions, and sometimes also the presence of inorganic structure directors.[18]

*Author to whom correspondence should be addressed. Fax: (+420)286-582-307. E-mail: jiri.cejka@jh-inst.cas.cz.

(1) Čejka, J.; Wichterlová, B. *Catal. Rev.* **2002**, *44*, 375.
(2) Maesen, Th. *Introduction to Zeolite Science and Practice*, 3rd Ed.; Čejka, J., van Bekkum, H., Corma, A., Schüth, F., Eds.; Studies in Surface Science and Catalysis 168; Elsevier: Amsterdam, 2007; pp 1−12.
(3) Čejka, J.; Vondrová, A.; Wichterlová, B.; Vorbeck, G.; Fricke, R. *Zeolites* **1994**, *14*, 147.
(4) Wichterlová, B.; Čejka, J.; Žilková, N. *Microporous. Mater.* **1996**, *6*, 405.
(5) Čejka, J.; Žilková, N.; Wichterlová, B.; Eder-Mirth, G.; Lercher, J. A. *Zeolites* **1996**, *17*, 265.
(6) Jones, C. W.; Zones, S. I.; Davis, M. E. *Microporous Mesoporous Mater.* **1999**, *28*, 471.
(7) Zheng, S.; Jentys, A.; Lercher, J. A. *J. Catal.* **2006**, *241*, 304.
(8) Rabiu, S.; Al-Khattaf, S. *Ind. Eng. Chem. Res.* **2008**, *47*, 39.
(9) Al-Khattaf, S.; Rabiu, S.; Tukur, N. M.; Alnaizy, R. *Chem. Eng. J.* **2008**, *139*, 622.
(10) Červený, L.; Mikulcová, K.; Čejka, J. *Appl. Catal., A* **2002**, *223*, 65.
(11) Botella, P.; Corma, A.; Navarro, M. T.; Rey, F.; Sastre, G. *J. Catal.* **2003**, *217*, 406.
(12) Datka, J.; Gil, B. *J. Mol. Struct.* **2001**, *596*, 41.
(13) Gil, B.; Zones, S.I..; Hwang, S. J.; Bejblová, M.; Čejka, J. *J. Phys. Chem. C* **2008**, *112*, 1997.
(14) Bevilacqua, M.; Meloni, D.; Sini, F.; Monaci, R.; Montanari, T.; Busca, G. *J. Phys. Chem. C* **2008**, *112*, 9023.
(15) Bisio, C.; Martra, G.; Coluccia, S.; Massiani, P. *J. Phys. Chem. C* **2008**, *112*, 10520.
(16) Nachtigall, P.; Bludský, O.; Grajciar, L.; Nachtigallová, D.; Delgado, M. R.; Areán, C. O. *Phys. Chem. Chem. Phys.* **2009**, *11*, 791.
(17) Grajciar, L.; Areán, C. O.; Pulido, A.; Nachtigall, P. *Phys. Chem. Chem. Phys.* **2010**, *12*, 1497.
(18) Čejka, J. Zeolites and ordered mesoporous materials: Progress and prospects. In *Proceedings of the 1st FEZA School on Zeolites*, Prague, August 20−21, 2005; Čejka, J., van Bekkum, H., Eds.; Studies in Surface Science and Catalysis 157; Elsevier: Amsterdam 2005; p 111.

Published on Web 05/04/2010

This led to the preparation 14-ring zeolites like CIT-5,[19] UTD-1,[20] SSZ-53 and SSZ-59,[21] 18-membered-ring ECR-34,[22] and ITQ-33[23] and 30-ring chiral ITQ-37.[24] Understanding of the templating behavior of organic structure-directing agents on a molecular level is still a matter of discussion and general conclusions have not yet been achieved. Fortunately, recent results showed a phase prediction in some synthesis of zeolites,[25] a deeper understanding of the interplay between guest organic cations and silicon oxide,[26] and also the role of supramolecular chemistry in the structure direction of microporous materials.[27] Further development and understanding of zeolite nucleation,[28] synthesis of novel materials with an odd number of Si atoms in channel openings,[29] and role of templates during the synthesis[30] leads then to further achievements in preparation of zeolitic materials[31] or new insight in their catalytic functions.[32] Acidic properties of individual types of zeolites with particular zeolite channels then control the catalytic behavior in different reactions.[13,33,34]

Recently, the first zeolites with intersecting 12- and 14-ring channels were reported as germanosilicates ITQ-15 and IM-12,[35,36] with their Si/Ge ratios being 8.5 and 4.5, respectively. As templates, 1,1,3-trimethyl-6-azonia-tricyclo-[3.2.1.4^{6,6}]decane hydroxide and (6R,10S)-6,10-dimethyl-5-azoniaspiro[4.5]decane hydroxide were used, respectively. Structural investigation evidenced that key structural building units are double 4-rings (D4R), the formation of which proceeds in the presence of Ge atoms in the reaction mixture[37−39] and is not limited only for UTL zeolite but also for other germanosilicate zeolites such as ITQ-22,[40] ITQ-17,[37] and ITQ-33.[23]

Our previous investigation addressed the critical synthesis parameters of germanosilicate of UTL topology, possessing 14 rings versus 12 rings.[41] (6R,10S)-6,10-Dimethyl-5-azoniaspiro[4.5] decane hydroxide was used as the structure-directing agent. The kinetics of the synthesis, the role of the Si/Ge ratio in the synthesis mixture, and the effect of calcination procedure were related to the crystallinity and textural properties of the synthesized zeolite. The optimum synthesis time was determined to be 6 days for Si/Ge and (Si + Ge)/SDA molar ratios of 2 and 1.7, respectively. The UTL zeolite crystallizes as small sheets 10 μm × 10 μm. The micropore volume of the best crystals was 0.23 cm^3/g.

The crystallization of ITQ-15 and IM-12 zeolites with UTL structure using SDA with different structures and basicity in a wide range of Si/Ge ratios shows a large variability of synthesis conditions for formation of this zeolite. It is obvious that, for the formation of the UTL structure, in a similar way as that for other germanosilicate zeolites, the space-filling role of the template is not the only dominating factor but the structure design of SBU units, typical for reaction mixtures with a Si/Ge ratio of 2, also plays a major role. Based on that, we assume the following:

- the nature of template is not the decisive factor for formation of UTL structure; however, the proper choice of the particular SDA is required;
- SDA used for synthesis of ITQ-15 and IM-12 is not unique, and probably is not the best for UTL crystallization;
- the presence of germanium, as an inorganic structure director, is definitely needed (at relatively high concentrations).Thus, some synergism between the presence of the particular organic SDA and inorganic director is of primary importance to prepare a well-crystalline zeolite of UTL structure.

The structure-directing agent with the inorganic component can determine the crystallization product. One of the ideas of our work was investigation of the template properties and hydrophilicity/hydrophobicity balance (log P), rigidity, basicity (pK_a), and their influence on the phase selectivity in germanosilicate reaction mixtures, from which UTL structure can be obtained. With respect to that, we used a series of spiroazacompounds with different structure and size to examine their structure-directing role in the synthesis of UTL structure.

Hence, we should solve such questions, as what are the limits of size, rigidity, solubility, basicity, etc. for quaternary nitrogen-containing molecules as potential structure-directing agents for synthesis of zeolites with UTL

(19) Wagner, P.; Yoshikawa, M.; Lovallo, M.; Tsuji, K.; Taspatsis, M.; Davis, M. E. *Chem. Commun.* **1997**, 2179.
(20) Lobo, R. F.; Tsapatsis, M.; Freyhardt, C. C.; Khodabandeh, S.; Wagner, P.; Chen, C. Y.; Balkus, K. J.; Zones, S. I.; Davis, M. E. *J. Am. Chem. Soc.* **1997**, *119*, 8474.
(21) Burton, A.; Elomari, S.; Chen, C. Y.; Medrud, R. C.; Chan, I. Y.; Bull, L. M.; Kibby, C.; Harris, T. V.; Zones, S. I.; Vittoratos, E. S. *Chem. Eur. J.* **2003**, *9*, 5737.
(22) Strohmaier, K. G.; Vaughan, D. E. W. *J. Am. Chem. Soc.* **2003**, *125*, 16035.
(23) Corma, A.; Díaz-Cabañas, M. J.; Jorda, J. L.; Martinez, C.; Moliner, M. *Nature* **2006**, *443*, 842.
(24) Sun, J.; Bonneau, C.; Cantín, A.; Corma, A.; Díaz-Cabañas, M. J.; Moliner, M.; Zhang, D.; Li, M.; Zou, X. *Nature* **2009**, *458*, 1154.
(25) Burton, A. W. *J. Am. Chem. Soc.* **2007**, *129*, 7627.
(26) Zones, S. I.; Burton, A. W.; Lee, G. S.; Olstead, M. M. *J. Am. Chem. Soc.* **2007**, *129*, 9066.
(27) Gomez-Hortiguela, L.; Lopez-Arbeola, F.; Cora, F.; Perez-Pariente, J. *J. Am. Chem. Soc.* **2008**, *130*, 13274.
(28) Itani, L.; Liu, Y.; Zhang, W.; Bozhilov, K. N.; Delmotte, L.; Valtchev, V. *J. Am. Chem. Soc.* **2009**, *131*, 10127.
(29) Corma, A.; Diaz-Cabanas, M. J.; Jorda, J. L.; Rey, F.; Sastre, G.; Strohmaier, K. G. *J. Am. Chem. Soc.* **2008**, *130*, 16482.
(30) Jackowski, A.; Zones, S. I.; Hwang, S. J.; Burton, A. W. *J. Am. Chem. Soc.* **2009**, *131*, 1092.
(31) Jeong, N. C.; Lee, Y. J.; Park, J.-H.; Lim, H.; Shin, C. H.; Cheong, H.; Yoon, K. B. *J. Am. Chem. Soc.* **2009**, *131*, 13080.
(32) Huang, J.; Jiang, Y.; Reddy Marthala, V. R.; Hunger, M. *J. Am. Chem. Soc.* **2008**, *130*, 12642.
(33) Žilková, N.; Bejblová, M.; Gil, B.; Zones, S. I.; Burton, A. W.; Chen, C.-Y.; Musilová-Pavlačková, Z.; Košová, G.; Čejka, J. *J. Catal.* **2009**, *266*, 79.
(34) Corma, A.; Llopis, F. J.; Martinez, C.; Sastre, G.; Valencia, S. *J. Catal.* **2009**, *268*, 9−17.
(35) Corma, A.; Díaz-Cabañas, M. J.; Rey, F.; Nicolopoulus, S.; Boulahya, Kh. *Chem. Commun.* **2004**, 1356.
(36) Paillaud, J.-L.; Harbuzaru, B.; Patarin, J.; Bats, N. *Science* **2004**, *304*, 990.
(37) Corma, A.; Navarro, M. T.; Rey, F.; Rius, J.; Valencia, S. *Angew. Chem., Int. Ed.* **2001**, *40*, 2277.
(38) Corma, A.; Navarro, M. T.; Rey, F.; Valencia, S. *Chem. Commun.* **2001**, 1720.
(39) Schaack, B. B.; Schrader, W.; Schüth, F. *Chem. Eur. J.* **2009**, *15*, 5920.
(40) Corma, A.; Rey, F.; Valencia, S.; Jorda, J. L.; Rius, J. *Nat. Mater.* **2003**, *2*, 493.
(41) Shvets, O. V.; Zukal, A.; Kasian, N.; Žilková, N.; Čejka, J. *Chem. Eur. J.* **2008**, *14*, 10134.

Table 1. Prepared Organic Compounds Used as Structure-Determining Agents (SDAs)[a]

N	SDA	C/N, 3°a + 4°a	pK_a	logP	δ_N^+	N	SDA	C/N, 3°a + 4°a	pK_a	LogP	δ_N^+
1		11, 2+1	12.40 ±0.03	–1.49 ±0.45	0.530	14	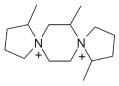	7.5, 3+2	12.52 ±0.05	–1.29 ±0.60	0.515
2	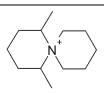	12, 2+1	12.19 ±0.03	–1.17 ±0.45	0.533	15	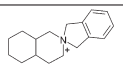	17, 6+3	11.82 ±0.04	0.01 ±0.47	0.546
3	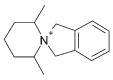	15, 6+3	11.89 ±0.03	–0.84 ±0.47	0.526	16	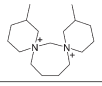	8.5, 2+2	12.11 ±0.03	-0.02 ±0.60	0.562 0.553
4		12, 3+1	12.45 ±0.04	–1.60 ±0.45	0.522	17	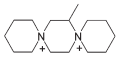	7.5, 1+2	12.01 ±0.04	–0.32 ±0.59	0.553 0.517
5		11, 2+1	11.90 ±0.03	–1.09 ±0.45	0.555	18	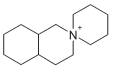	14, 2+1	12.26 ±0.04	–0.14 ±0.45	0.571
6		12, 2+1	11.84 ±0.04	–0.77 ±0.45	0.566	19	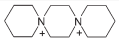	7, 0+2	12.03 ±0.04	–0.32 ±0.59	0.534 0.534
7	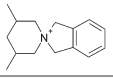	15, 6+3	11.76 ±0.03	–0.62 ±0.47	0.545	20		11, 0+1	12.10 ±0.03	–0.63 ±0.44	0.557
8		12, 3+1	12.01 ±0.03	–1.20 ±0.45	0.544	21		9, 2+2	11.85 ±0.04	0.30 ±0.60	0.551 0.554
9		14, 2+1	11.86 ±0.03	–0.42 ±0.45	0.562	22		14, 0+3	12.61 ±0.05	–1.29 ±0.60	0.524
10	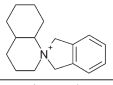	17, 6+3	11.74 ±0.04	–0.28 ±0.47	0.533	23	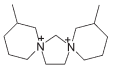	7, 2+2	12.06 ±0.04	0.04 ±0.60	0.550 0.556
11	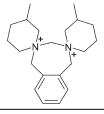	10, 4+4	12.14 ±0.03	0.64 ±0.67	0.544	24	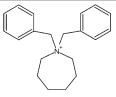	20, 10+3	11.57 ±0.05	0.99 ±0.47	0.544
12		12, 1+1	12.15 ±0.03	–0.93 ±0.44	0.544	25		17, 13+4	11.62±0.05	2.22 ±0.69	0.553 0.555
13	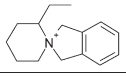	15, 2+3	11.84 ±0.03	–1.78 ±0.46	0.529						

[a] 3°a + 4°a: denotes the quantity of tertiary and quaternary C and N atoms, as a measure of rigidity/flexibility of a molecule, designation according to ref 38. δ_N^+ denotes the efficient charge for nitrogen ions calculated using semiempirical method PM3 (program Hyperchem Pro 6).

structure. In addition, we tried to elucidate peculiarities of crystallization processes of UTL zeolite using different templates, especially regarding crystallization kinetics and product phase selectivity. To solve the problem of synergism of organic and inorganic structure-directors, a series of nitrogen-containing compounds (mainly spiroazaalkanes), presented in Table 1 were synthesized using oil−water interphase alkylation reactions promoted by NaOH (see Scheme 1) and tested as SDA for zeolite synthesis from germanosilicate mixtures with a Si/Ge ratio of 2.

Experimental Section

Materials and Methods. *Synthesis of the Template*. In general, the preparation of structure-directing agents (SDAs, see Scheme 1) was performed using a method similar to that described in ref 42, with subtle variations, depending on the nature (primarily the solubility) of obtained substances. Typically, 140 mL of distilled water, 5.68 g of sodium hydroxide, and 30.66 g of 1,4-dibromobutane (or equivalent molar quantity of another bromoderivate) were mixed in a glass flask. An amount of 16.07 g of (2R,6S)-2,6-dimethylpiperidine (or equivalent molar quantity of another cyclic amine) was added dropwise over a period of 30 min under reflux. Then, the mixture was refluxed under very intensive stirring (∼1000

(42) Electronic supplementary information available via the Internet: http://www.rsc.org/suppdata/cc/b4/b406572g/.

(43) Camblor, M. A.; Barrett, Ph.A.; Díaz-Cabañas, M.-J.; Villaescusa, L. A.; Puche, M.; Boix, T.; Pérez, E.; Koller, H. *Microporous Mesoporous Mater*. **2001**, *48*, 11.
(44) Conradsson, T.; Zou, X.; Dadachov, M. S. *Inorg. Chem*. **2000**, *39*, 1716.
(45) Li, Y.; Zou, X. *Angew. Chem., Int. Ed*. **2005**, *117*, 2048.

Scheme 1. General Scheme of the Preparation of Spiroazacompounds as Structure-Directing Agents (SDAs)

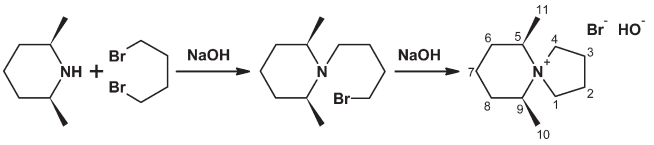

rpm) for 12 h to prepare a milklike suspension and then cooled in an ice bath. After adding 70 mL of an ice-cooled 50 wt % solution of sodium hydroxide, different quantities of solid sodium hydroxide were added under intensive stirring and cooling by ice until the appearance of oil product. As a rule, after 0.5−1 h of stirring, this oil crystallized. When no crystallization proceed over an extended period of time, the reaction mixture was additionally cooled by means of liquid nitrogen (the stark oil was separated mechanically) and solid produced was filtered off and extracted with 1−5 100-mL amounts of chloroform. The organic fractions were dried by anhydrous sodium sulfate and partially evaporated and the ammonium salt was precipitated and washed out with diethyl ether. Finally, the salts were converted to hydroxide form by ion-exchange with AG 1-X8 resin (Bio-Rad). The yield of the product, depending on the structure, was about 34−96%. The successful synthesis of the SDA was confirmed by ^{1}H NMR spectra after dissolution in dimethyl-sulfoxide-d_6. A list of all templates under study, with their characteristics, is given in Table 1.

Cyclic amines and bromoderivatives used for the synthesis of SDAs:

(2R,6S)-2,6-dimethylpiperidine, 3,5-dimethylpiperidine (mixture of *cis* and *trans*), 2,2,6,6-tetramethylpiperidine, decahydroquinoline (mixture of *cis* and *trans*), perhydroisoquinoline, 1,1′-methylenebis(3-methylpiperidine), hexamethyleneimine, piperazine, 2-methylpiperazine, 2-ethylpiperidine; 1,4-dibromobutane, 1,5-dibromopentane, 1,4-dibromopentane, α,α′-dibromo-o-xylene, 1,2-dibromoethane, (1-bromoethyl)benzene.

The compounds were obtained in pure forms, because none of them is commercially available. Their structures were confirmed by ^{1}H NMR. In many cases, identification of the compound structures was difficult, because of presence of several isomers (up to 8 for template 8). As an example, for template 1, the peak identification in ^{1}H NMR spectra was made as follows:

- H10 and H11 — doublet 1.287 and 1.309 ppm, $I \approx 6$
- H6 and H8 — two multiplets, at 1.499−1.643 ppm, $I \approx 4$
- H7 — two pentaplets with centers at ∼1.729 and 1.767 ppm, $I \approx 1 + 1$
- H2 and H3 — pentaplets with centers at ∼1.925 ppm, $I \approx 4$
- H5 and H9 — multiplets at 3.301−3.350 ppm, $vI \approx 2$,
- H1 and H4 — two multiplets 3.555−3.676 ppm, $I \approx 4$Here, the total number of protons is −22; the impurities include H_2O (3.322 ppm) (∼5%), and the rest represents < 1%.

We measured pH for 0.005−0.01 N mixtures of all obtained templates in their OH forms and used the data to calculate experimental values pK_a (presented in Table 1) as a degree of template basicity. For calculation, we used classical methodology based on Debye−Hückel theory:

$$pK_a = 14 - pK_b = 14 + \log(K_b) \quad (\text{at } 25°C)$$

$$K_b = \frac{[SDA^+] \times [OH^-]}{[SDAOH]} = \frac{[OH^-]^2}{c - [OH^-]}$$

$$= \frac{((a_{OH^-})^2/(\gamma_{OH^-})^2)}{c - (a_{(OH^-)}/(\gamma_{OH^-}))} = \frac{10^{2pH-28}/(\gamma_{OH^-})^2}{c - (10^{pH-14}/(\gamma_{OH^-}))}$$

where c is the concentration of SDA determined by potentiometric titration, a the activity, and γ the activity coefficient. For very diluted solutions with

$$\sqrt{I} < 0.1 (c < 0.01 \text{ N})$$

the activity coefficient was determined as a first approximation:

$$\log \gamma = -A \times \left| z^{SDA+} \times z^{OH^-} \right| \times \sqrt{I}$$

where A is a constant (which is equal to 0.505 for water solutions), z the charge number of the ion concerned, and I the ionic strength of the solution.

The efficient charge for N ions was calculated using the semiempirical method PM3 (program Hyperchem Pro 6). Similarly, log P values (n-octanol/H_2O distribution coefficient, program ChemSketch 12.01) were calculated for characterization of the degree of hydrophobicity of the templates.

Preparation of the UTL/X Zeolites. The preparation of the UTL/X zeolites was performed using methods similar to those previously published.[42] A gel with the molar composition 0.6−1.0 SiO_2:0.6−0.2 GeO_2:0.2−0.7 ROH:30−33 H_2O was prepared by dissolving amorphous (or crystalline) germanium oxide (Aldrich) in a SDA hydroxide (ROH) solution. Silica (Cab-O-Sil M5) then was added to the solution and the mixture was stirred at room temperature for 30 min. The resulting fluid gel was charged into 30-mL Teflon-lined autoclaves and heated at 175 °C for 3−14 days under agitation (40 rpm). The solid products obtained after preset synthesis times were recovered by filtration, washed with distilled water, and dried overnight at 90 °C. To remove the SDA, the as-synthesized zeolites were calcined in a stream of air at 550 °C for 6 h with a temperature ramp of 1 °C/min.

A detailed description of the synthesis of samples UTL/14 and UTL/16 is provided as follows.

UTL/14. 2.344 g of SDA9 has been dissolved in 11.3 mL of water. To this solution, we have added 4 g of ion-exchange resin AG 1-X8 and placed the resulting mixture on a magnetic stirrer for 2 h. After that, the resin was separated by filtration. To the obtained solution, 0.872 g of amorphous germanium oxide was added and the gel

was stirred for 15 min to fully dissolve. Then, 1.000 g of silica (Cab-O-Sil M5) was added into the solution and the mixture was stirred at room temperature for 30 min. The resulting fluid gel was charged into 30 mL Teflon-lined autoclaves and heated at 175 °C for 9 days under stirring (40 rpm). The solid product was recovered by filtration, washed out with distilled water, and dried overnight at 90 °C.

UTL/16. 11.9 mL of SDA11 (2,10-dimethyl-15,16-benzo[*a,a*]-6,8-diazoniadispiro [5.1.5.4]heptadecane hydroxide) solution has been mixed with 1.0 mL of water. To the obtained solution, 0.872 g of germanium oxide was added and mixed for 15 min before full dissolution of the germanium oxide. Then, 1.000 g of silica (Cab-O-Sil M5) was added into the solution and the mixture was stirred at room temperature for 30 min. The resulting fluid gel was charged into 30-mL Teflon-lined autoclaves and heated at 175 °C for 4 days under agitation (40 rpm). The solid product was recovered by filtration, washed out, and dried overnight at 90 °C.

Characterization. Powder X-ray diffraction (XRD) data were obtained on a Bruker AXS D8 diffractometer in the Bragg−Brentano geometry using Cu Kα radiation with a graphite monochromator and a position-sensitive detector (Vantec-1). Relative crystallinity of individual zeolite samples was determined using the diffraction line at 6.23° with a (*hkl*) index of (200). To limit the effect of preferential orientation of individual UTL crystals, a gentle grinding of the samples to decrease their size and careful packing into the holder was performed.

The content of silicon and germanium was determined on a Philips PW 1404 Model X-ray fluorescence spectrometer. Zeolite samples after calcination were homogenized using an agate mortar and, after adding dentacryle as binder, they were deposited on a surface of cellulose tablets.

The morphology of zeolite particles was evaluated using scanning electron microscopy (SEM) (JEOL Model JSM-5500LV).

FTIR spectra of skeletal vibrations of UTL samples were recorded on a Fourier transform infrared (FTIR) spectrometer (Nicolet Model Protégé 460), using a KBr pellet technique.

Thermogravimetric analysis (TGA) and differential thermal analysis (DTA) were performed on a Model Q-1000 thermal analyzer (MOM, Hungary) from room temperature to 1000 °C with a heating rate of 10 °C/min under flowing air.

Adsorption isotherms of argon and nitrogen at −196 °C were measured with a Micromeritics ASAP 2020 instrument. Prior to the adsorption measurements, all samples were degassed at 250 °C until a pressure of 0.001 Pa was attained. Nitrogen and argon were used as adsorbates to properly evaluate the pore size of this microporous germanosilicate. Micropore size distribution was calculated using density functional theory (DFT)[46] and Saito−Foley[47] methods for cylinder pore geometry.

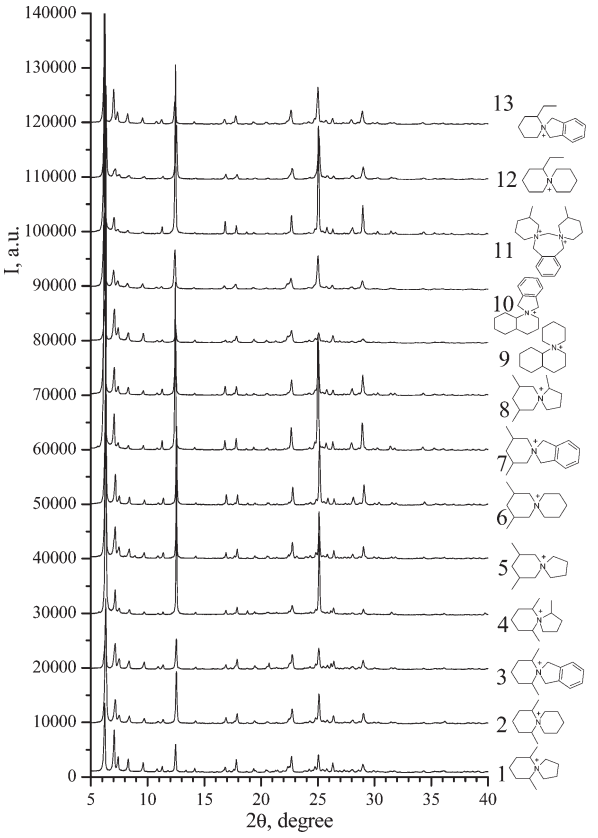

Figure 1. XRD spectra of samples with UTL structure synthesized in the presence of different templates.

^{1}H (300 MHz) NMR spectra used for characterization of the prepared SDA were recorded on a Varian Mercury 300 spectrometer in dimethyl sulfoxide-d_6 solutions at 25 °C (data are not shown here).

Results

The use of 13 of the 25 tested SDAs, together with the appropriate composition of the reaction mixture, and under proper synthesis conditions, led to the formation of highly crystalline zeolites with UTL topology (see Figure 1 and Table 2). Negligible differences in XRD patterns of samples prepared using different templates can, most probably, be related to little differences in sample degree of crystallinity and crystal size (the possibility of some preferential orientation of sheetlike crystals in the sample holder[41]), as well as different populations of germanium and silicon in different crystallographic sites.

At ratios of Si/Ge = 2 and (Si + Ge)/SDA = 1.7−4 in the reaction mixture, the optimum duration of the synthesis was 6 days for most of the zeolites, whereas when decreasing the Si/Ge ratio to 1 (sample UTL 6a), pure product was obtained after 3 days of synthesis. Similarly, an essential reduction of hydrothermal synthesis time was observed when using SDA5 and SDA11. In the former case, it is associated with a smaller template molecule size

(46) Lowell, S., Shields, J. E., Thomas, M. A., Thommes, M., *Characterization of Porous Solids and Powders: Surface Area, Pore Size and Density*; Kluwer, Dordrecht, The Netherlands, 2004; pp 145, 148.

(47) Saito, A.; Foley, H. C. *AIChE J*. **1991**, *37*, 429.

Table 2. SiO_2-GeO_2 Samples: UTL and Other Structures Using Different Templates

	Molar Ratio in RM									
sample	Si	Ge	Te	H_2O	Si/Ge in RM	(Si + Ge)/Te in RM	template number	synthesis duration	primary phase	impurities (%)
UTL/1	0.80	0.40	0.3	30	2	4	1	6	UTL	
UTL/2	0.80	0.40	0.7	30	2	1.7	1	6	UTL	
UTL/2a	0.80	0.40	0.7	30	2	1.7	1	4	UTL	
UTL/3	0.80	0.40	0.4	30	2	3	1	6	UTL	
UTL/4	0.80	0.40	0.6	30	2	2	1	6	UTL	
UTL/5	1.00	0.20	0.4	30	5	3	1	6	UTL	
UTL/6	0.60	0.60	0.4	30	1	4	1	6	UTL	β-GeO_2, 10
UTL/6a	0.60	0.60	0.4	30	1	4	1	3	UTL	
UTL/7	0.80	0.40	0.5	30	2	2.4	6	6	UTL	
UTL/8	0.80	0.40	0.6	30	2	2	2	6	UTL	
UTL/9	0.80	0.40	0.6	30	2	2	5	4	UTL	
UTL/10	0.80	0.40	0.2	30	2	2	3	8	UTL	
UTL/11	0.80	0.40	0.45	30	2	2.67	7	6	UTL	
UTL/12	0.80	0.40	0.6	30	2	2	8	6	UTL	
UTL/13	0.80	0.40	0.4	30	2	3	4	6	UTL	
UTL/14	0.80	0.40	0.5	30	2	2.4	9	9	UTL	
UTL/15	0.80	0.40	0.2	30	2	6	10	7	UTL	
UTL/16	0.80	0.40	0.2	30	2	6	11	4	UTL	
UTL/17	0.80	0.40	0.4	30	2	4	12	6	UTL	
UTL/18	0.80	0.40	0.3	30	2	4	13	6	UTL	
UTL/19	0.80	0.40	0.185	30	2	6.5	14	9	MEL	UTL, 10, amorph.
UTL/20	0.80	0.40	0.25	30	2	4.8	14	6	MTW	UTL, 5
UTL/21	0.80	0.40	0.222	30	2	5.4	15	6	UTL	BEA, 40, amorph.
UTL/22	0.80	0.40	0.344	30	2	3.5	15	14	MTW	UTL, 10, amorph.
UTL/23	0.80	0.40	0.4	30	2	3	16	6	UTL	MTW, 10
UTL/24	0.80	0.40	0.3	30	2	4	16	7	MTW	UTL, 20
UTL/25	0.80	0.40	0.3	30	2	4	17	6	amorph	UTL

and the absence of shielding of the N atom by methyl groups. A smaller template size and the absence of shielding could make the interaction of positively charge N atoms and negative silica species easier. In the latter case, we assume that high values of pK_a and log P for a rather big SDA molecule (containing two charged N atoms) are of the utmost importance. Also, it is impossible to exclude the possible decomposition of molecule SDA11 (with rupture of the methylene group between N atoms), because of a longer hydrothermal treatment. Flexible products of decomposition of SDA11 can be formed, initiating the formation of medium-pore-size zeolite with MEL structure.

Although, in most cases, highly crystalline samples were synthesized over a wide (Si + Ge)/SDA ratio, it can be stressed that zeolites crystallized from reaction mixtures that have higher template contents exhibited more perfect structure and a higher micropore volume. In contrast, when using large SDA molecules (SDA3, SDA7, SDA10, and SDA11), decreasing the template contents (Si + Ge)/SDA = 6 were necessary. It is possibly caused by, essentially, the great volume of these molecules, and unattainability of appropriate filling of zeolite pores by the large molecules, because of steric hindrances.

The optimum pH range for the successful synthesis of highly crystalline UTL zeolites was 9.0−11.5. In some cases, a decrease in pH to 8.5 (for SDA7), 8.0 (for SDA12), 7.5 (for SDA3), and even to 6.5 (for SDA1) still led to a well-crystalline UTL zeolite. It can be expected that, in the case of reaction media with lower pH, a prolongation of the synthesis time is required (from 3 days to 8 days) to achieve full crystallization of UTL zeolites. With some SDA applied (e.g., SDA9), even at pH 9.5, 9−10 days were required to achieve complete crystallization. The large size and insufficient basicity and hydrophilicity of SDA molecules most probably caused a slower rate of UTL zeolite crystallization. Increasing the pH to 12.0 or even higher resulted in recrystallization that occurred too fast, resulting in less-porous zeolites, which is typical for silicate media.

We did not observe any direct correlation between the properties of templates and their ability to favor the formation of zeolites with topology UTL. At the same time, we noticed that all SDAs applied for successful synthesis of UTL zeolites possess some similar characteristics, which will be discussed in more detail vide infra. Here, we just propose limits of optimum and acceptable values for those characteristics. All SDAs successfully applied for UTL synthesis exhibit C/N values in the range of 10−17, the values of pK_a are in the range from 11.74 ± 0.02 to 12.45 ± 0.04, and the calculated values of log P are between 1.78 ± 0.47 and 0.64 ± 0.67 (see Table 1, as well as Figures 5 and 6 (presented later in this work).

For most of these 13 SDAs, a slight deviation from the optimum synthetic conditions led to significant changes in the direction of crystallization, providing some impurities or undesired zeolite phases. Using, e.g., SDA5, a prolongation of the hydrothermal synthesis from the optimum 4 days to 6 days caused crystallization of zeolite MEL, whereas a decrease in the template content to 50% in the reaction mixture (decreasing the pH in the reaction mixture from 9 to 6) initiated the formation of highly crystalline β-GeO_2 and amorphous phase SiO_2. We observed such phenomenon each time the pH value of the reaction medium was not sufficiently high (the limit most probably depends on the nature of the SDA and the

SDA/(Si + Ge) ratio) to involve the recrystallization process of silica and germanate species in the same way. This can be explained in terms of a partial overlapping of precipitation fields for silicate and germanate polyanions. For most SDAs, when the pH is <8.5, only germanate species are crystallized. Thus, the silicate species remain in the amorphous gel.

For SDA10, a increase in the template content in the reaction mixture of ~50% of the original optimum value caused the transformation of a substantial part of the primary formed UTL phase into a denser MTW zeolite. We assume that the reason for such a transformation is not only due to faster crystallization of the UTL phase and its subsequent transformation, according to the Ostwald ripening rule, but also displacement of the equilibrium of the dissolution/sedimentation of germanate and silicate species (because of essential increase pH) in favor of the increase in the silica contents in a solid phase. Similarly, for SDA11, a prolongation of synthesis time from the optimum 4 days to 5 days led to the formation of zeolite BEA further to UTL. For SDA9, traces of BEA zeolite appeared with increasing the synthesis time from 9 days to 10 days.

For SDA14−SDA17, we did not succeed in optimizing the synthesis conditions to prepare UTL zeolite as a pure phase. SDA14, SDA15, and SDA16 represent a group of SDAs, in the presence of which UTL zeolite crystallized; however, the UTL structure was always accompanied by other zeolitic structures. SDA15 provides UTL as the dominating phase, with BEA zeolite as the impurity. With increasing the synthesis time up to 14 days, MTW becomes the dominating phase and the UTL phase is found only as an impurity. In comparison, for SDA16, together with the dominating UTL phase, the impurity was MTW zeolite if the synthesis time was 6 days, but MTW/UTL phases were formed for syntheses of 7 days or more. The use of SDA14 led to the formation of small quantities of the desired UTL zeolite; however, the main phase were zeolites with MEL and/or MTW structures. With SDA17, only a small amount of UTL phase was formed; the major part of the sample was amorphous, even at prolongated synthesis times.

The following issues should be noted when considering the reasons why specified templates are not "successful" in the synthesis of pure zeolites with UTL topology. The structures of SDA14 and SDA17 are rather similar, but the first one possesses high hydrophilicity (log $P = -1.29$) and basicity, whereas the second one, having a high pK_a value, is rather hydrophobic (log $P = -0.32$). As a consequence, the use of SDA14 causes not only very fast crystallization of the UTL zeolite but also fast transformation of this structure into a denser phase. We will notice that the final samples with UTL, MEL, and MTW phases contain very insignificant quantities of organic templates; that is, medium- and large-pore zeolites do not include SDA molecules in channels. SDA17 possesses insufficient templating ability, because of low hydrophilicity. At pH 9.0−9.5, we found only traces of crystallization UTL zeolite, whereas the increase of pH to 10.5−11.0 leads to the formation of the porous MTW phase. One cannot exclude that the use of this template (SDA17) could be successful in obtaining a pure UTL phase only under very careful control of pH (e.g., by balancing concentrations of OH^-/Br^- in a solution) and at prolonged synthesis times. SDA16 also possesses insufficient templating ability, because of low hydrophilicity, but at a higher pK_a value. Therefore, we observe a fast transformation of the UTL structure in MTW.

It is necessary also to note that SDA16 consists of several isomers, because of the structure of the initial amine, and it also brings some disbalance. The basic feature of SDA16 (besides sufficiently high hydrophobicity) is its adverse corner (close to 135°, unlike SDA10, where this corner is ~90°), placing two sufficiently bulky substituents, favoring the formation of zeolites with the BEA structure.

Templates SDA18 and SDA20 were also favorable for the formation of the BEA mixture with an unknown phase. SDA18 is a structure analogue of SDA16 with similar chemical properties; therefore, the reasons for the formation of BEA zeolite are almost identical. The ability of simple small azaspirocompounds similar to SDA20 to promote the formation of zeolites with BEA topology is shown in ref 43. For successful templating of UTL structures for the SDA20 molecule, obviously a lack of methyl or ethyl group attached to the carbon next to quaternary nitrogen is critical. In the case of SDA19 and SDA21 (which are very similar to SDA17 and SDA16), the main products were zeolites with MTW topology. With SDA16−SDA19 and SDA21, potential instability (vide infra) in the conditions of synthesis also should be considered.

In the presence of SDA22 and SDA23, we were not able to optimize the synthetic conditions to form any zeolite structure. The main reason can be both too-fast crystallization of quartz (and β-GeO_2) as well as thermal instability of SDAs. In the case of SDA24 and SDA25, visible evidence showed that an absence of zeolitization is caused by both very high hydrophobicity and flexibility of molecules.

SEM images of UTL zeolites prepared using SDA1 in the synthesis mixture (Figure 2a) showed that, after 4−6 days of the hydrothermal synthesis at a temperature of 175 °C, homogeneous, rectangular (close to square) sheetlike crystals <0.5 μm thick and with an average size of ~10 μm × 10 μm were formed. For zeolites prepared with SDA1, a majority of crystals are isolated ones, while a minority of them consists of aggregates of lamellar crystals. Note that SEM, together with powder XRD, confirms a high degree of crystallinity and phase purity of the prepared samples of UTL zeolites. The resulting morphology of the crystals under study differs from the morphology of IM-12 crystals described by Paillaud et al.[36] The authors reported on the formation of two types of crystals: large aggregates 150 μm × 150 μm × 150 μm in size, under static synthesis conditions, and flower-type aggregates of thin crystals under agitation.

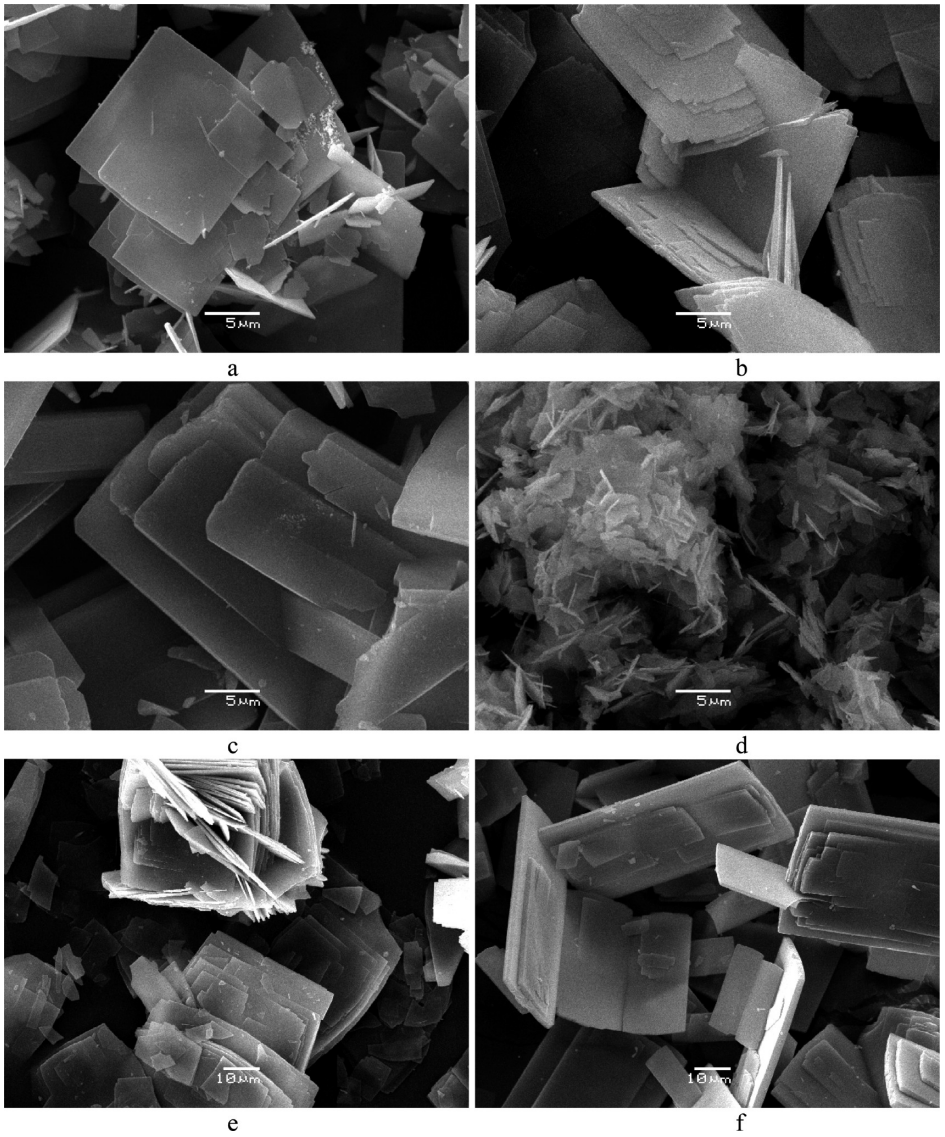

Figure 2. SEM images of samples with UTL topology: (a) UTL/2−SDA1, (b) UTL/8−SDA2, (c) UTL/11−SDA7, (d) UTL/14−SDA9, (e) UTL/15−SDA10, and (f) UTL/19−SDA14.

UTL zeolites prepared in the presence of other SDAs possess the morphology of rectangular sheetlike crystals (see Figures 2b−2f). In general, it is seen that, first of all, SDA type influences the crystal homogeneity. By changing the SDA, a very broad variety of crystal sizes (1−60 μm in the planar direction and with a thickness of 0.1−4 μm), different ordering of separation of crystal sheets, as well as degree of perpendicular or planar intergrowth, can be obtained. It should be stressed that larger crystals were formed in the presence of larger SDAs (i.e., SDA7 and SDA13) with benzene rings in the structure (Figure 2c and 2f). These SDAs are less soluble in water having higher pK_a values. It can be speculated that these factors favor a low rate of nuclei formation and a relatively fast growth of isolated UTL crystals. In some cases, we also observed the formation of "open book" type crystal aggregates (see Figure 2e).

For better understanding of the reaction conditions leading to the pure well-crystalline UTL zeolite, we followed the kinetics of all successful syntheses (see Figure 3). For some SDAs (especially for SDA5 and SDA11), some diffraction lines typical of UTL structure appeared already after 1 day of the synthesis at 175 °C. The intensity of these diffraction lines increased with the prolongation of the synthesis time and it seems that the maximum intensity (optimum synthesis time under reaction conditions used) is ~3−7 days (depending on SDA type, cf. Table 1). Further prolongation of the synthesis time behind the optimum one for each SDA led to the appearance of diffraction lines of other, more-dense, zeolites with MTW, MEL, or BEA. After 6−12 days of synthesis (depending on the SDA applied), more-dense zeolite is the prevailing material in the reaction mixture, whereas, after 14 days, quartz is preferentially formed.

Figure 3 provides a scheme of the time evolution of the content of UTL, MTW, and α-quartz (+ β-GeO_2) phases in the synthesis products. All zeolites identified in the synthesis products (UTL and MTW, MEL, or BEA) represent intermediates in this reaction system prepared

with an optimum synthesis time of ~3−7 days for UTL. Crystallization kinetic of zeolites with UTL topology is particularly dependent on the SDA being used. Thus, significant acceleration of crystallization in comparison with SDA1, narrowing the time window of pure UTL phase and quick phase transformation into MTW or BEA correspondingly, are typical features of SDA5 and SDA11. The only similarity in these two SDAs is the absence of alkyl groups close to the central charged N atom. In contrast, the employment of SDA3 and SDA7 particularly prolonged the induction period of UTL crystallization and shifted the time window of UTL phase to 8−9 days. The general phase diagram of zeolite with UTL topology, depending on the SDA type being transformed in a more-dense structure, is illustrated in Figure 4.

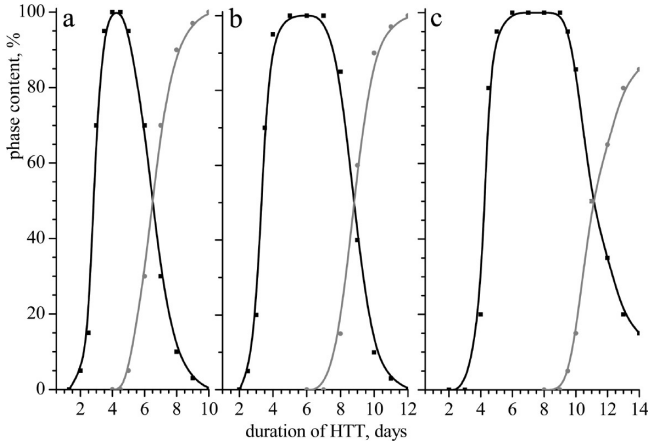

Figure 3. Kinetics of crystallization for zeolite with UTL topology (black line) synthesized in the presence of different SDA: SDA5 (pattern (a)), SDA1 (pattern (b)), and SDA9 (pattern (c)). (For patterns a, b, and c, the black line denotes UTL and the gray line represents MEL data.)

FTIR spectra of the skeletal vibration region for zeolite with the UTL structure, synthesized with different SDAs, are very similar, which allows us to draw a conclusion about the insignificant influence of the template nature on the zeolite framework vibrations. The assignment of the infrared bands was mainly based on refs 44 and 45. The spectra show the presence of intensive stretching absorption bands at 1171 and 1241 cm^{-1} and bending vibrations at 525, 539, 578, and 594 cm^{-1} (see Figure SI-1 in the Supporting Information). No significant redistribution of the intensities of pair bands at 525 and 539 cm^{-1} and 578 and 594 cm^{-1} was observed for zeolites synthesized in the presence of different SDAs. In addition, even using synchrotron radiation, we were not able to locate individual templates in the structure of UTL zeolites synthesized with different SDAs. This indicates no additional significant deformations of the zeolite framework as a

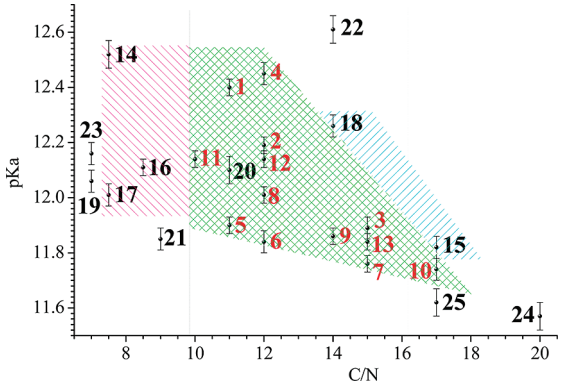

Figure 5. Influence of C/N ratio and pK_a of SDAs (numbers given in the graph denote SDAs; see Table 1) on the formation selectivity of zeolites with UTL topology. (Green-shaded regions indicate areas where UTL formation is favorable; blue- and pink-shaded regions represent areas where UTL formation is bearable.)

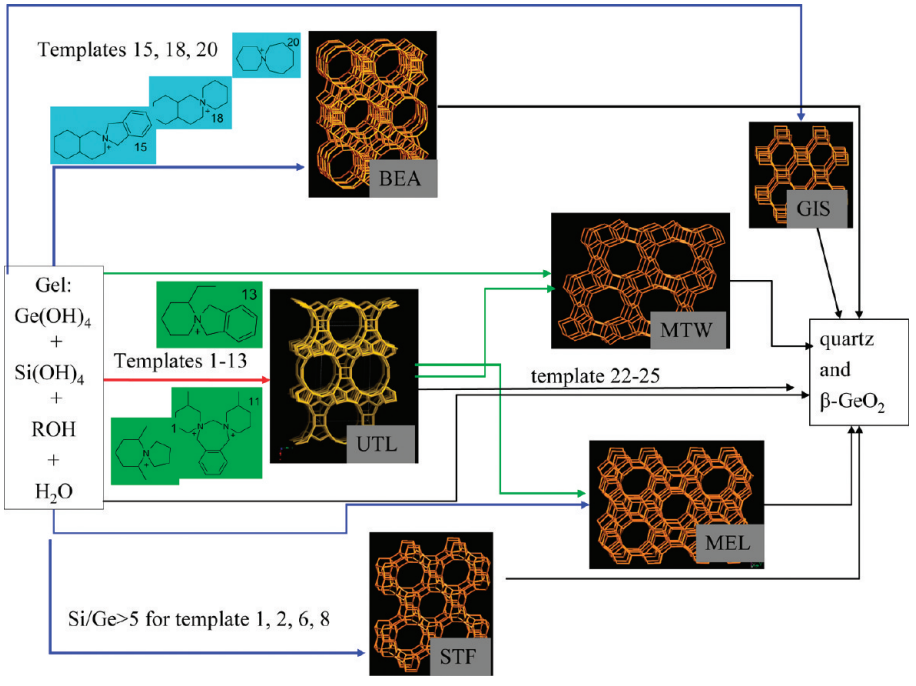

Figure 4. Phase transformation of zeolite with UTL topology in a more-dense structure.

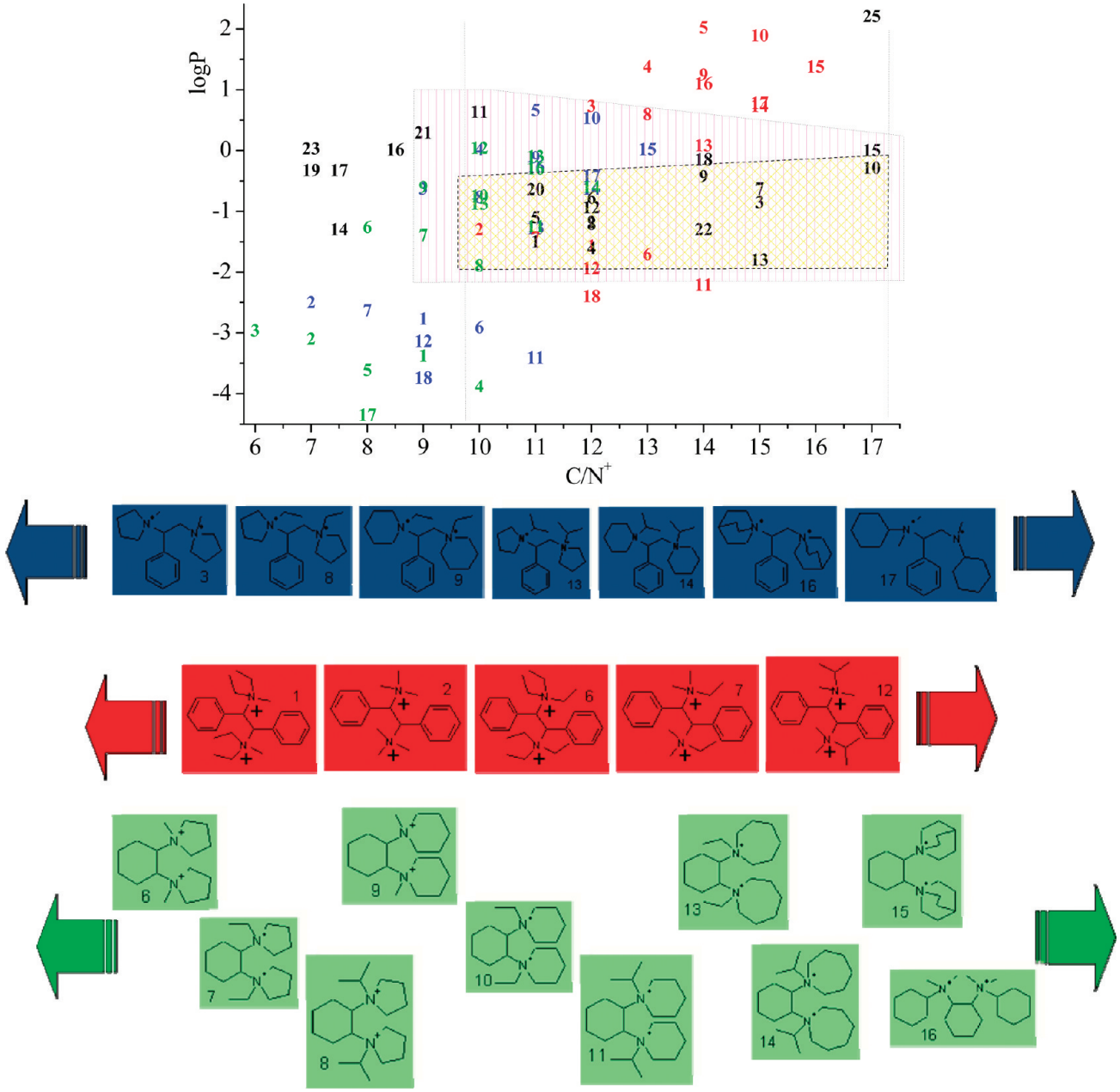

Figure 6. Field of optimum values of C/N ratio and log *P* for nitrogen-containing organic molecules suitable for use as SDAs in the synthesis of large-pore and extra-large-pore zeolites from silicate and germanosilicate media. Black numbers represent SDA numbers from this work; blue, red, and green numbers in the graph represent SDAs from the figures below the graph. The yellow field denotes the region of desirable values, and the magenta field denotes the admissible limits of the C/N ratio and log *P*.

change of the distribution of silicon and germanium in the framework. This is probably related to the preferential location of Ge atoms in the D4R units.[37] A shoulder in the spectrum found at 980 cm^{-1} could be assigned to the vibrations including Si−O−Ge moieties and four absorption peaks at 930−835 cm^{-1} associated with different type Ge−O−Ge species, most probably located in D4R units. For as-synthesized zeolites, the specified changes in a FTIR spectrum reflect, first of all, changes of type and intensity of absorption bands attributed to C−H and C−N vibration of the template (in particular, in the case of the presence of aromatic groups, e.g., for SDA3, SDA7, SDA10, SDA11, SDA13, SDA15, SDA24, and SDA25).

The thermogravimetric analysis (TG, DTG) and differential thermal analysis (DTA) results of UTL zeolites synthesized from two different SDAs are rather similar and are shown in Figure SI-2 of the Supporting Information. Generally, for all samples, the weight loss happens in two steps. The first step is observed in the temperature range from ambient temperature up to 300−350 °C (depending on the type of SDA). This weight loss is due to the desorption of water from the zeolite. The second step in the range from 300 up to 700 °C corresponds to the SDA removal. Further weight loss above 700 °C is obviously caused by a partial dehydroxylation of UTL zeolites. Zeolites with UTL structure show very high thermal stability; their structure did not collapse, even

after calcinations up to 1000 °C. Note that the temperature range of the dehydration depends on the Si/Ge ratio and can be explained by different surface hydrophobicity of the zeolite. In contrast, the temperature corresponding to the maximum of template removal is somewhat different for all UTL zeolites under study. As-synthesized zeolite prepared with SDA containing aromatic rings show an additional maximum at 650−680 °C, which is attributable to the oxidation of aromatic hydrocarbon moieties.

Textural parameters of the porous structure of the UTL zeolites were determined using adsorption isotherms with nitrogen and argon as adsorbates (see Figures SI-3 and SI-4 in the Supporting Information). The BET surface area was 660−720 m^2/g. The micropore volume of crystalline zeolite samples prepared with different SDAs agrees well with the total amount of template and water in the as-synthesized samples (and CHN analysis data) and was intended to average 0.21−0.23 cm^3/g. For example, in the case of not well-crystalline samples UTL/2a (4 days of synthesis) and UTL/5, the micropore volume was 0.152 and 0.155 cm^3/g, respectively (at template contents of 12.73 and 12.60 wt %, water contents of 3.36 and 2.81 wt %, Si/Ge ratios of 4.18 and 9.44, the calculated free space will be 0.175 and 0.167 cm^3/g). For better crystalline samples (UTL/2 and UTL/7), the void volume was 0.220 and 0.213 cm^3/g, respectively, practically not depending on the SDA type.

The analysis of N_2 and Ar adsorption isotherms in the pressure range from $p/p_0 = 10^{-6}$ up to $p/p_0 = 4 \times 10^{-1}$ allowed us to determine the micropore size distributions for calcined samples. For the determination based on nitrogen adsorption isotherms, the DFT approach[46] and the Saito−Foley[47] method estimated the average pore diameter close to 1.05 and 1.10 nm, respectively.[41] The analysis of the Ar adsorption isotherm using the Saito−Foley (SF) method provided a diameter of ~1.20 nm (see Figure SI-4 in the Supporting Information). It is well-known that the pore diameter is very sensitive, with respect to the values of the magnetic susceptibility and polarizability.[46] Argon is usually preferred, because of its spheric shape; however, the value obtained from argon measurements is higher than that from powder XRD. It is important to note that only one maximum has been obtained, even without any shoulder. This indicates that even a high-resolution argon measurement is unable to distinguish between two types of UTL pores with diameters of 8.5 Å × 5.5 Å and 9.5 Å × 7.1 Å. Although the pore diameters determined, based on Ar and N_2 adsorption isotherms, are slightly overestimated, they are in relatively good agreement with the XRD analysis data. Both confirm that the investigated zeolites possess extra-large pores.

Discussion

Analyzing the peculiarities of the crystallization of UTL zeolites in the presence of different SDAs and trying to explain the influence of the template nature on the crystallization process and phase selectivity of products some important factors are discussed in relation to Figure 5.

The Basicity of SDA Molecules, Containing Positively Charged Quarternary Nitrogen Atom(s). Experimentally definable pK_a values properly characterize the degree of dissociation of the pair cationic form of template/hydroxide ion, or the ionic strength of SDA as alkali (creation of some pH value of water solutions at adjusted concentration) can be a measure of the basicity. pK_a values that are too high (such as that for SDA22) accelerate the fast crystallization reaction, cause considerable displacement of a balance of SiO_2, and promote GeO_2 dissolution in favor of a more-complete dissolution of the germanium compounds. As a result, unfavorable conditions for the formation of UTL zeolite favor a quick crystallization process, leading to the preferential formation of quartz. Reducing the synthesis temperature to 130−150 °C, which is intended to prolong the synthesis time, did not result in the synthesis of pure UTL phase. pK_a values below optimum ones (admittedly 11.0−11.5) lead not only to excessive slowing of the crystallization (and to an increase in the probability of nucleus formation of other phases, e.g., with SDA21) but also to the insufficient dissolution and recrystallization of silica components (as a result, a majority of the solid phase formed will be found to be amorphous). The absence of any correlations between a calculated positive charge on the N atom and value of pK_a can be thus inferred (see Table 1). It is obvious that the local environment of the N atom is not the unique factor that determines the basicity of such a molecule. The C/N ratio is also of the utmost importance, as well as molecular weight, type and positions of substituting groups, and, also, probably conformation.

Balance of Hydrophobicity/Hydrophilicity of the SDA Molecule. Experimentally definable or calculated log *P* value (log *P* is defined as the ratio of the concentration of a compound in the aqueous phase relative to the concentration of this compound in an immiscible solvent, as the neutral molecule, usually the *n*-octanol/H_2O distribution coefficient) is a measure of the hydrophobicity/hydrophilicity of molecules.[48] To use the pH-dependent *n*-octanol/H_2O distribution coefficient, log *D* (log *D* = log *P* − log[1 + 10^(−charge × (pK_a − pH))]) is more correct when charged molecules are considered. One of the main factors (but not the only one) that determines a balanced hydrophobicity/hydrophilicity in SDA molecules is the C/N ratio. Gies and co-workers were the first to investigate the influence of the template structure (size and shape) on the crystallization of high-silica zeolites.[49] Kubota et al.[50] observed a correlation between template C/N^+ values, phase transfer behavior, and the ability for structure direction in zeolite synthesis. The authors also reported a simple method for determining the relative hydrophobicity of templates and observed a correlation

(48) Leo, A.; Hansch, C.; Elkins, D. *Chem. Rev.* **1971**, *71*, 525.
(49) Gies, H.; Marler, B. *Zeolites* **1992**, *12*, 42.
(50) Kubota, Y.; Helmkamp, M. M.; Zones, S. I.; Davis, M. E. *Microporous Mater.* **1996**, *6*, 213.

between the relative hydrophobicity and rigidity of the organic cations and their structure direction ability for the formation of high-silica zeolites. In this way, rigid molecules with intermediate hydrophobicity (10%−50% transport of tetraalkylammonium compounds from water to chloroform[51]) can be the best SDAs for the formation of new high-silica zeolites. The authors also noticed that organic SDAs for the successful synthesis of high-silica zeolites had, as a rule, C/N ratios in the range of 10−16. Based on that, it was reported that the transport of tetraalkylammonium compounds from water to chloroform indicated that molecules with a C/N^+ ratio of <10 strongly prefer water and the molecules with a C/N^+ ratio of >16 strongly prefer chloroform. Goretsky and coworkers[52] discussed the influence of hydrophobicity/hydrophilicity for various quaternary ammonium molecules and, accordingly, differences in their structure-directing role for ZSM-5 formation and concluded that the control of the hydrophobicity of the organic SDA is necessary for the synthesis of pure-silica zeolites.

As depicted in Figure 5, SDAs that are successful for UTL crystallization are generally included in this range. When some of the C atoms are aromatic instead of aliphatic, the appropriate C/N ratio can be higher (e.g., C/N = 17 for SDA10). The obvious reason is a higher hydrophilicity of aromatic compounds, because of the presence of π-orbitals in the SDA molecule. From Table 1, it follows that the optimum (calculated) values of log P for SDAs which are successful for UTL formation are in a wide range: −1.78 to −0.28 (±0.46). For SDA24, SDA25, and SDA15, the increasing C/N ratio (and, correspondingly, the increasing hydrophobicity, log $P > -0.2$) will lead to a decreased solubility of SDA molecules in water. This will not favor the formation of a hydrate shell around a SDA molecule (the formation of such an ordered, hydrophobic hydration sphere around the organic cation is an important intermediate stage in the process of zeolite crystallization[53]). The intermediate hydrophobicity of organic molecules permits their solubility in aqueous solution. In the limited space of the liquid phase among the colloidal particles of the gel, SDA hydrophobic hydration spheres and hydrophobically hydrated domains of soluble silicates could impact with each other and cause overlap of the hydration sphere to happen. The release of water molecules from the ordered hydrophobic hydration sphere into the bulk and the subsequent establishment of favorable van der Waals' contacts between alkyl chains of SDA and the hydrophobic silica could thus provide the entropic and enthalpic driving forces for the formation of the composite inorganic−organic species. The solvent shell of water molecules around the template can be displaced by a shell of less-polar silicate species to establish favorable van der Waals interactions. This assembly mechanism was proposed Burkett and Davis,[53,54] who also claimed that an intermediate template hydrophobicity is required for appropriate structure direction. It is proposed that the properties of organic molecules should balance the hydrophilic properties—to be soluble in water but not interact too strongly with water molecules. Simultaneously, they should provide a hydrophobic character that generates favorable interactions with the silica host but still be able to form a hydrate shell around them. For example, the authors of ref 55 showed that no crystalline product was obtained using tetraethylammonium cations, because they can participate in the hydrogen bonding network of water not forming a hydrophobic hydration sphere.[56] They concluded that the formation of a hydrophobic hydration sphere is significant to the mechanism of structure direction. The tetrapenthylammonium cation is an example of the opposite function: they tend to aggregate and phase-separate in aqueous solutions, rather than exist as isolated, hydrophobically hydrated cations.[57]

For SDA14, SDA16, SDA17, SDA19, SDA21, and SDA23, all of which contain two N atoms in the molecule, a decrease in the C/N ratio leads to the formally calculated values of log $P = -1.3$ to 0.3 obviously unequally represent the change in hydrophilicity, and it is necessary to use the log D value, which depends substantially on pH. It is worthwhile to stress that having the same overall formula of the SDA molecule, its hydrophobicity and basicity can be changed by a substitution of alkyl group type and their positions, with respect to the N atoms (cf. compare pairs SDA1/SDA5, SDA2/SDA6, and SDA4/SDA8 in Table 1 and Figure 4), as well as the position of the N atom in the individual structures (SDA9/SDA18, SDA10/SDA15). Obviously, limiting appropriate values of pK_a, log P (or log D), and C/N ratios are not strict during the changes of synthesis conditions and compositions of reaction mixtures. Successful synthesis of UTL zeolite is also possible with templates that also have boundary values of these parameters (e.g., with templates SDA14, SDA15, SDA16, and SDA17).

Size and Geometric Form of the SDA Molecule. The size and geometric form of templates under discussion play an important role in the synthesis of UTL zeolite, although, for UTL structures, no straightforward relationship between the volume and the size of channels and the size and volume of related SDA molecules was observed. This is supported by our XRD study not showing a specific location of SDA molecules in the channel system of UTL. The influence of geometry becomes apparent, first of all, in the case of conformationally rigid templates used for UTL structures when the geometry of bulky template molecules corresponds to the geometry of the UTL channels. For example, as for SDA9 and SDA10, well-crystalline UTL phases were synthesized while, with

(51) Zones, S. I.; Nakagawa, Y.; Rosenthal, J. W. *Zeoraito* **1994**, *11*, 81.
(52) Goretsky, A. V.; Beck, L. W.; Zones, S. I.; Davis, M. E. *Microporous Mater*. **1999**, *28*, 387.
(53) Burkett, S. L.; Davis, M. E. *J. Phys. Chem*. **1994**, *98*, 4647.
(54) Burkett, S. L.; Davis, M. E. *Chem. Mater*. **1995**, *7*, 920.
(55) Burkett, S. L.; Davis, M. E. *Chem. Mater*. **1995**, *7*, 1453.
(56) Wen, W. Y. In *Water and Aqueous Solutions*; Horne, R. A., Ed.; Wiley−Interscience: New York, 1972; p 613.
(57) Nakayama, H.; Kuwata, H.; Yamamoto, N.; Akagi, Y.; Matsui, H. *Bull. Chem. Soc. Jpn*. **1989**, *62*, 985.

SDA15, a UTL/BEA mixture is formed and, for SDA18, BEA and unknown phase(s) were obtained. However, this effect may not appear in a clear form, because these pairs of templates, which have the same overall formula, also differ in terms of basicity and hydrophilicity. Templates that are too large do not allow the formation of the UTL structure (for example, SDA24 and SDA25); however, here, the situation is complicated by a harsh increase in hydrophobicity, as well as excessive flexibility of structures.

Flexibility/Rigidity of Template Molecule. Under the same synthesis conditions, conformationally more rigid SDAs are more preferable, because they induce strict conditions for the formation of certain channel structures identically and do not allow any formation of more-compact zeolitic frameworks with smaller channels. Kubota et al.[50] examined three types of templates, as a function of SDA properties, and showed that bulky, rigid molecules with limited conformational variability are able to direct the unique formation of a great variety of new high-silica zeolites (SSZ-13, SSZ-23, SSZ-25, SSZ-26, SSZ-31, SSZ-33, and SSZ-37). The use of relatively flexible molecules with a minimum diameter of 5 Å that more loosely fit into 12-ring pores gives more than one molecular sieve. The authors of ref 50 also have noted that many tertiary and quaternary atoms in the template skeleton can serve as a measure of rigidity. The fewer the number of choice of conformations, the easier the prediction of the form and pore size of zeolite. This will be discussed in more detail vide infra. It indicates that, for successful synthesis, the number of atoms and their positions in SDA are more important than the absolute number of the atoms (in the main body of molecule or in the opposite borders of flexible molecule). At the same time, it is obvious that aromatic rings possess higher rigidity: 5-rings are more rigid than 6- or 7-rings and are especially more rigid than a linear chain of C atoms. The flexibility of SDA may strongly affect the selectivity of the synthesis. Linear amines or polyamines gave one-dimensional zeolites, such as TON or ZSM-48, while branched amines generally prefer the formation of zeolites with multidimensional pore systems (such as MFI or MEL).[58] Rigid SDAs may be more selective, in comparison with flexible molecules, which can achieve a higher number of conformations. However, there are some examples, when rigid molecules such as *N*,*N*,*N*-trimethyladamantammonium was favorable for the crystallization of five different zeolites (SSZ-13, SSZ-23, SSZ-24, SSZ-25, SSZ-31).[58] Furthermore, there are some flexible molecules (both linear and branched) that produce only one or a few phases (e.g., TPA and TBA).

Thermal and Hydrothermal Stability of the Template. Retaining the SDA structure at least until the end of the formation of a zeolite structure is required. It is known that molecules containing one methylene group between two N atoms are not stable enough. For example, diaminomethane is not sufficiently stable[59] in the monopronated or unprotonated forms in a water solution, even at room temperature. Such substances in alkaline media, even in nonaqueous media, decompose with ammonia evaluation (Hoffmann degradation). So, diaminomethane dihydrochloride in dioxane in the presence of Et_3N is used as a slow ammonia-releasing agent.[60] Certainly, more assistance at N atoms, including N atoms in 5- or 6-rings, as well as the existence of charge on N atoms, will stabilize such compounds. However, bond breakage in SDA molecules under hydrothermal conditions cannot be completely excluded. While, in the case of SDA11, the availability of benzene rings obviously stabilizes the SDA molecule (as a result, with this template, the formation of zeolites with UTL topology is possible), then for SDA16, SDA21, SDA25, and especially SDA23, we are uncertain of the invariance of the template's structure during the entire hydrothermal synthesis time. The formation of smaller or more linear molecules favorable to constituting zeolites with smaller pore diameters can be the result of the destruction of SDAs. This can be evidenced by the following example of such a template transformation in the synthesis of FOS-5 zeolite, as shown in ref 61. Those authors reported, but did not explain, the reasons and the mechanism of transformation in an alkali solution of enough stable molecules of 1,4-diaza-bicyclo-[2,2,2]-octane into two molecules of trimethylamine with a necessary breakage of three relatively strong C−C bonds.

All SDAs that were successfully used for the synthesis of UTL zeolites possess C/N values in a range of 10−17; the pK_a values calculated from experimental data are between 11.74 ± 0.02 and 12.45 ± 0.04, and the calculated log *P* value fit into the interval between -1.78 ± 0.47 and -0.64 ± 0.67 (see Table 1 and Figure 5). The knowledge and understanding of the acceptable limits of C/N and log *P* values can help with preliminary selection of potentially "successful" SDAs in the synthesis of large and extra-large pore zeolites from silicate and germanosilicate synthesis media from a variety of nitrogen-containing organic compounds and to predict their templating ability (see Figure 6). Because of the possible synthesis of such compounds and the admissible flexibility of their structures, this will allow a more purposeful search for new SDAs to be performed.

Thus, in this contribution, we reported on a clear synergism between the optimum structure and properties (pK_a, log *P*) of organic templates and the presence of a critical amount of inorganic component (GeO_2) for crystallization of zeolite with UTL topology. We stress that, for the formation of this structure, there are the following optimum conditions of the synthesis mixture: Si/Ge = 2, (Si + Ge)/SDA = 3, pH 10.5−11, and, using SDAs, the organic molecules containing one or two quaternary N

(58) Burton, A. W.; Zones, S. I. *Stud. Surf. Sci. Catal.* **2007**, *168*, 137.
(59) Knudsen, P. *Chem. Ber.* **1914**, *47*, 2698.
(60) Galaverna, G.; Corradini, R.; Dossena, A.; Marchelli, R. *Int. J. Pept. Protein Res.* **1993**, *42*, 53.
(61) Conradsson, T.; Dadachov, M. S.; Zou, X. D. *Microporous Mesoporous Mater.* **2000**, *41*, 183.

atoms (C/N ratio = 10−17) with an optimum hydrophobicity/hydrophilicity balance (log $P = (-1.78 \pm 0.47) - (0.64 \pm 0.67)$) and basicity ($pK_a = 11.74 \pm 0.02 - 12.45 \pm 0.04$). Some templates from those investigated by us allow expansion in this area of formation of pure UTL structure, up to a Si/Ge ratio of 1−5 in the reaction mixture by an appropriate optimization of other synthesis parameters (e.g., a change of hydrothermal treatment duration). The use of other SDAs allows the performance of hydrothermal zeolite synthesis in a wide pH range (6.5−11.5) or at essentially lower concentrations of SDA in the reaction mixture. At the same time, zeolites with UTL topology cannot be obtained according to our present understanding from reaction mixtures with a Si/Ge ratio less than 1 or more than 5 (this is possibly associated with a key role of Ge atoms in the formation of D4R secondary building units) or, using templates, the C/N, pK_a, and log D values, which are outside the specified limits.

Conclusions

Several silicogermanate zeolites with UTL topology have been synthesized in basic media using 13 different structure-directing agents (SDAs) in hydroxide form as SDAs. The optimum synthesis time was determined to be 3−7 days at a Si/Ge ratio of 2 and (Si + Ge)/SDA molar ratios of 1.7−6. Zeolite with UTL structure shows very high thermal stability: the structure does not collapse after calcinations, even at 1000 °C. The micropore volume of the best crystals is 0.21−0.23 cm^3/g, and the micropore diameter, based on nitrogen and argon adsorption experiments, is ∼1.0 nm. The influence of the composition of the reaction mixture, template nature (structure, hydrophilicity/hydrophobicity balance, rigidity/flexibility, pK_a) on the phase selectivity, degree of crystallinity, and adsorption properties of zeolites with UTL structure were established and discussed. On the basis of the experimental data received in this work, selection criteria of organic molecules (from a family of nitrogen-containing bases) as potential SDAs in the synthesis of large and extra-large pore zeolites from silicate and germanosilicate media are offered. These criteria can be summarized as follows:

(1) The organic molecule, potentially successful as SDA in the synthesis of high-silica or germanosilicate zeolites, should contain, in the structure, one or two quaternary N atoms and have a C/N ratio in the range of 10−16. The inclusion of one or two benzene rings into the structure of SDA connected with nitrogen not less than through one CH_2 group is acceptable. In this case, the C/N values can be even 17 to 18.

(2) The SDA molecule should possess sufficient rigidity. It is desirable that its structure includes two or more 5- or 6-membered aliphatic hydrocarbon rings. Spiro-structure, especially with a charged N atom in a place joining two rings, as well as the presence of benzene rings, is useful.

(3) The SDA molecule should possess optimum hydrophobicity. Based on our study and literature data, calculated log P values in the range between −1.8 and −0.6 are desirable. In contrast, the presence of oxygen atoms or other heteroatoms in a molecule is undesirable.

(4) The SDA should possess sufficiently high stability under the conditions of hydrothermal synthesis of zeolites. Presence of one bridged methylene group between two charged N atoms, as well as the aromatic quaternary N atom in the SDA structure, is undesirable.

(5) The kinetic diameter of a SDA molecule should be within the following limits: 7−15 Å.

Acknowledgment. Financial support of the Grant Agency of the Czech Republic is highly appreciated (projects 104/07/0303 and 203/08/0604).

Supporting Information Available: Figures describing FTIR of skeletal vibrations of as-synthesized samples with UTL topology prepared with using SDA2-1 and SDA3-2, SDA5-3, SDA7-4, and SDA 6-5 (Figure SI-1); thermogravimetric analysis of as-synthesized UTL samples prepared using SDA1-1 and SDA3-2 (Figure SI-2); adsorption isotherms of nitrogen for samples of UTL zeolite (see Tables 1 and 2) prepared using SDA1-1 and SDA6-2 (Figure SI-3); and adsorption isotherms of argon and pore-size determination for samples of UTL/6, UTL/7, UTL/14, UTL/16 zeolites prepared with using SDA1-1, SDA6-2, SDA9-3, and SDA11-4 (Figure SI-4). This material is available free of charge via the Internet at http://pubs.acs.org.